Early Archaean Microorganisms Preferred Elemental Sulfur, Not Sulfate

Pascal Philippot, *et al.*

Science **317**, 1534 (2007);
DOI: 10.1126/science.1145861

Early Archaean Microorganisms Preferred Elemental Sulfur, Not Sulfate

Pascal Philippot,[1]* Mark Van Zuilen,[1] Kevin Lepot,[1] Christophe Thomazo,[1] James Farquhar,[2] Martin J. Van Kranendonk[3]

Microscopic sulfides with low $^{34}S/^{32}S$ ratios in marine sulfate deposits from the 3490-million-year-old Dresser Formation, Australia, have been interpreted as evidence for the presence of early sulfate-reducing organisms on Earth. We show that these microscopic sulfides have a mass-independently fractionated sulfur isotopic anomaly ($\Delta^{33}S$) that differs from that of their host sulfate (barite). These microscopic sulfides could not have been produced by sulfate-reducing microbes, nor by abiologic processes that involve reduction of sulfate. Instead, we interpret the combined negative $\delta^{34}S$ and positive $\Delta^{33}S$ signature of these microscopic sulfides as evidence for the early existence of organisms that disproportionate elemental sulfur.

The availability and speciation of sulfur in the Archaean atmosphere-ocean system must have played an important role in the early evolution of life on Earth. The different oxidation states of this element (e.g., S^{2-}, S^{-}, S^0, $S_2O_3^{2-}$, SO_3^{2-}, SO_4^{2-}) can all act as an important source of energy for different types of sulfur-metabolizing organisms. It has been suggested that the large sulfur isotopic fractionation of sulfides (e.g., pyrite, FeS_2) in marine sediments relative to contemporaneous sulfate [e.g., gypsum ($CaSO_4$) or barite ($BaSO_4$)] provides a record of microbial sulfate reduction over time (*1*–*7*), because sulfate-reducing organisms preferentially process light over heavy sulfur isotopes (^{32}S relative to ^{34}S), leading to sulfide minerals (e.g., pyrite) with negative $\delta^{34}S = \{[(^{34}S/^{32}S)_{sample}/(^{34}S/^{32}S)_{std} - 1] \times 1000\}$ values (*8*). The resulting isotopic difference between sulfides and sulfates ($\delta^{34}S_{sulfide} - \delta^{34}S_{sulfate} = -20$ to -30‰) can be traced back to 2700 to 2500 million years ago (*3*, *5*). In older rocks, a much smaller isotopic difference is preserved ($\delta^{34}S_{sulfide} - \delta^{34}S_{sulfate} < -10$‰), which could indicate either that microbial sulfate reduction was absent in the Early Archaean or that microbial sulfate reduction operated under low seawater-sulfate concentration (*7*). These low sulfate concentrations would be consistent with low oxygen concentrations in the Archaean atmosphere and surface ocean (*6*, *7*). An exception to this general trend, however, is the record of strongly negative $^{34}S/^{32}S$ values of microscopic sulfides hosted in barite of the 3490-million-year-old chert-barite deposit at North Pole [Dresser Formation, Western Australia (*1*, *2*)]. It has therefore been suggested that the record of microbial sulfate reduction extends into the Early Archaean and may reflect local enrichment of sulfate in these environments (*1*).

Here we report multiple–sulfur isotope analyses (^{32}S, ^{33}S, ^{34}S) of sulfides and sulfates from drill-core samples from the chert-barite deposit at North Pole and show that metabolic pathways other than sulfate reduction can account for the microscopic sulfides with negative $^{34}S/^{32}S$ values. In the anoxic and strongly hydrothermally influenced marine environment of the Early Archaean, organisms using reduced to intermediate forms of sulfur such as S^0, $S_2O_3^{2-}$, and SO_3^{2-} were likely more common than sulfate-reducing organisms (*9*, *10*). Sulfides that form from the metabolism of S^0, $S_2O_3^{2-}$, and SO_3^{2-} may also result in significantly lower $^{34}S/^{32}S$ ratios relative to abiologic forms of sulfide (*11*). This mass-dependent isotope fractionation ($\delta^{34}S$) therefore cannot be used to distinguish such organisms from SO_4 reducers. However, in the Archaean, the different sources of sulfur used by these organisms carry distinctive mass-independent isotope ratios {anomalous $\Delta^{33}S = 1000 \times [(1 + \delta^{33}S/1000) - (1 + \delta^{34}S/1000)^{0.515}]$} (*12*–*14*). Such $\Delta^{33}S$ anomalies are produced by photochemical reactions of volcanic gases (SO_2 and H_2S) in the Archaean atmosphere and have been recognized as a tracer of the source of sulfur on early Earth (*12*–*14*). The $\delta^{34}S$ and $\Delta^{33}S$ variations for the Early Archaean record appear to be well matched by experiments of atmospheric photolysis undertaken with ultraviolet (UV) radiation of wavelength ~193 nm (*13*). In Late Archaean sediments, however, Ono *et al.* (*15*) and Kamber and Whitehouse (*16*) documented a different relation between $\delta^{34}S$ and $\Delta^{33}S$ variations and showed that their data could be bracketed by experiments undertaken with 193-nm radiation and by experiments undertaken at longer wavelengths (>220 nm) (*12*–*14*). The data for the Mesoarchaean produces another relation between $\delta^{34}S$ and $\Delta^{33}S$, adding to the complexity of the picture and raising the possibility that the interpretations of (*13*) and (*15*, *16*) may be reconciled if they reflect changes in the source reactions that occurred as the atmospheric sulfur cycle evolved from the Early Archaean to the Late Archaean. These different scenarios for atmospheric photochemical reactions suggest that S^0 and SO_4 will dominate over all other sulfur species and provide two notable sulfur sources, insoluble S^0 ($+\Delta^{33}S$) and soluble SO_4 ($-\Delta^{33}S$), that are available for sulfur metabolism. Once the $\Delta^{33}S$ anomaly is passed on to a given reservoir, it will be preserved unless there is addition of sulfur with a different $\Delta^{33}S$ composition. Figure 1 illustrates how sulfides that formed from different microbial processes would retain the $\Delta^{33}S$ anomaly of the original sulfur source.

The Dresser Formation at North Pole consists of pillowed and komatiitic metabasalt interleaved with three units of cherty metasediment. Our study focuses on the lowermost of these metasedimen-

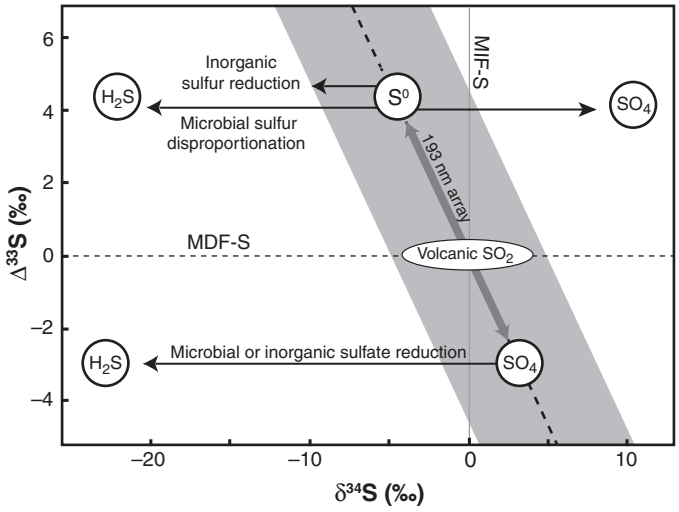

Fig. 1. Graphical representation of multiple–sulfur isotope systematics in a $\delta^{34}S$ versus $\Delta^{33}S$ plot. UV-driven photolysis of volcanic SO_2 and H_2S produces aerosols and gases (H_2S, HS, S^0, SO_2, SO_3, H_2SO_4) with both mass-independent (MIF-S, $\Delta^{33}S$) and mass-dependent isotope fractionations (MDF-S, $\delta^{34}S$) that follow experimentally determined fractionation arrays for UV radiation of 193 nm (shaded area represents a margin in $\delta^{34}S$ of ±5‰ relative to this array) (*13*). The dominant atmospheric carriers of $\Delta^{33}S$ anomalies are elemental sulfur aerosols (S^0, $+\Delta^{33}S$) and sulfuric acid aerosols (H_2SO_4) incorporated in seawater as dissolved sulfate (SO_4, $-\Delta^{33}S$). Sulfide forming from the biologic or abiologic reduction of sulfate should preserve a negative $\Delta^{33}S$ anomaly. Likewise, sulfides formed by the inorganic or microbial reduction of elemental sulfur should retain a positive $\Delta^{33}S$ anomaly, whereas microbial disproportionation of elemental sulfur should produce sulfide and sulfate that both retain a positive $\Delta^{33}S$ anomaly. Isotope fractionation associated with microbial sulfur reduction is close to zero (*26*) and therefore not shown.

[1]Equipe Géobiosphère Actuelle et Primitive, Institut de Physique du Globe de Paris, CNRS and Université Denis Diderot, 4 place Jussieu, 75005 Paris cedex, France. [2]Earth System Science Interdisciplinary Center, Department of Geology, University of Maryland, College Park, MD 20742, USA. [3]Geological Survey of Western Australia, 100 Plain Street, East Perth, WA 6004, Australia.

*To whom correspondence should be addressed. E-mail: philippot@ipgp.jussieu.fr

tary units known as the chert-barite unit (Fig. 2A). The age of this unit is constrained by a Pb-Pb age on galena from barite (*17*). The rocks were deposited in a shallow-water environment, possibly within a volcanic caldera (*18*, *19*), and have experienced low-grade metamorphism between 100° and 350°C (*19*). The unit consists of a succession of bedded cherts, bedded barite, volcanoclastic sandstones, and bedded carbonates. It is connected to an underlying network of barite- and silica-feeder veins. The barite veins, like the silica veins, are thought to represent conduits for hydrothermal fluid circulation (*19*–*21*). In the bedded barite, massive barite crystal fans alternate with centimeter-scale, macroscopic sulfide laminates (Fig. 2C). The barite crystals from both the bedded barite and underlying intrusive barite veins contain microscopic sulfides (Fig. 2D). The chert-barite unit has a history of complex hydrothermal alteration that is characterized by successive pulses of fluid circulation as attested by widespread silica, carbonate and sulfide overgrowth of primary textures. Several zones of relatively unaltered barite crystals, however, were found in the barite beds. We selected microscopic sulfide arrays from such unaltered barite for textural analysis [sample 88-4 of drill core Pilbara Drilling Project 2B (PDP2B)] (Fig. 2D) and sulfur-isotope and chemical analyses (samples 84-6, 89-3 of drill core PDP2B, and sample 96-6 of drill core PDP2C) (Fig. 3C and fig. S1) (*22*). Some of these microscopic sulfides in the bedded barite have up to 3.5 weight % Ni, and can contain local inclusions of pentlandite $(Fe,Ni)_9S_8$ and millerite (NiS) (fig. S1 and table S1). Specific tests with Ni-sulfide standards during the analytical procedure (*22*) show that Ni content, or the occurrence of pentlandite or millerite, has a negligible effect on sulfur-isotope analysis. Furthermore, no correlation between Ni content and $\delta^{34}S$ is present in the data set.

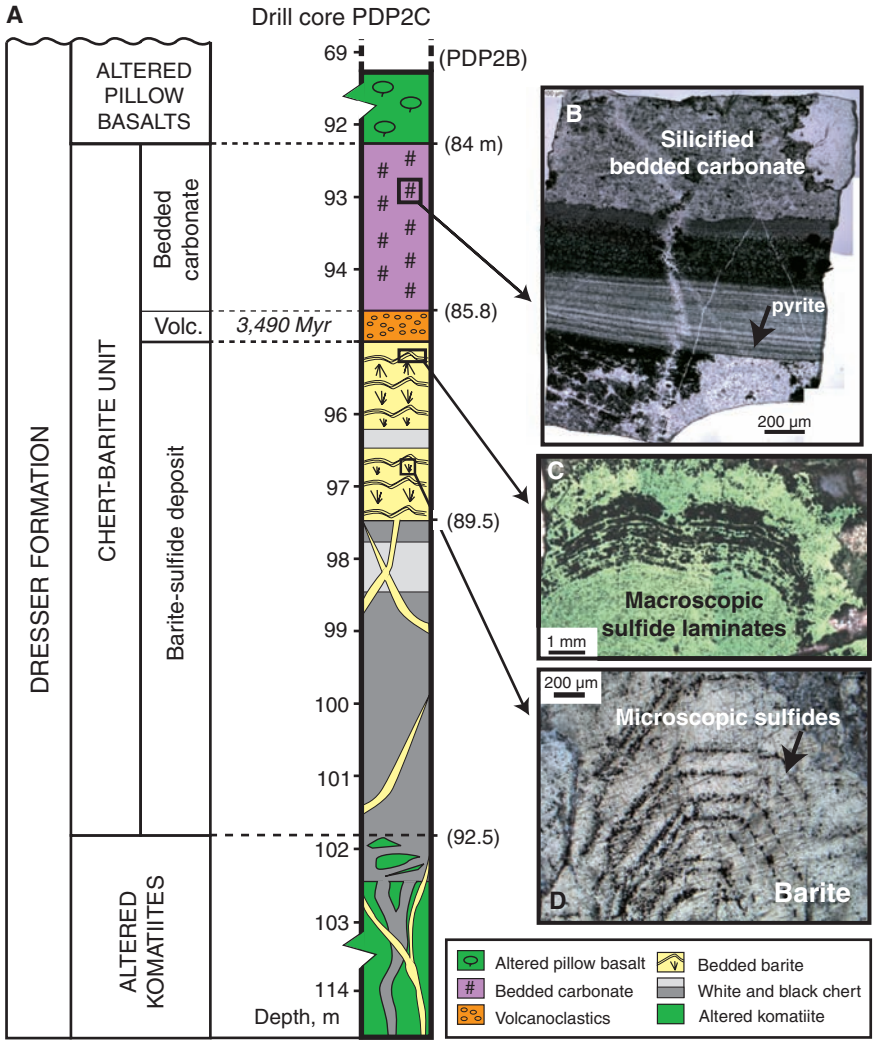

Fig. 2. (**A**) Lithological log of the Pilbara Drilling Project (*36*) for drillcore PDP2C. Five main subunits have been identified, but only three are shown for simplification. Numbers in parentheses (on the right) refer to depths (m) at which drill core PDP2B intersected the three main subunits. These include, from bottom to top, (i) hydrothermally altered komatiites intruded by silica and barite veins, (ii) barite-sulfide deposit, and (iii) volcanoclastic sandstone (Volc.) and bedded carbonate sedimentary rocks overlain by pillowed basalts. (**B** to **D**) Optical photomicrographs. (B) Silicified bedded carbonate containing thin alignments of sedimentary sulfide (sample 94.6, drill core PDP2C). (C) Macroscopic sulfide laminates (sample 95.35, drill core PDP2C). (D) Individual barite crystal containing microscopic sulfides lining barite overgrowth zones (sample 88.4, drill core PDP2B).

Our $\delta^{34}S$ data (*22*) (Fig. 3, fig. S2, and tables S2 and S3) show a limited range of values for sedimentary sulfides in the volcanoclastic sandstones and bedded carbonates (−1.4 ± 2.7‰) and macroscopic sulfide laminates in the bedded barite (−2.7 ± 1.2‰). By contrast, microscopic sulfides occurring in several barite crystals of one of the well-preserved zones within the bedded barite (fig. S1; zones 89-3a I, II, III, and zone 89.3b of drill core PDP2B) are strongly fractionated and have $\delta^{34}S$ values as low as −22.6‰. The $\delta^{34}S$ values overlap with those of previous studies, in which the mean $\delta^{34}S$ of macroscopic sulfide laminates (−0.9 ± 1.5 and −2.4‰ ± 0.8) were interpreted as unfractionated volcanogenic sulfur (*1*, *23*), and highly ^{34}S-depleted microscopic sulfides within bedded barite between −1.3 and −16.8‰ were attributed to sulfate-reducing microorganisms (*1*).

Our $\Delta^{33}S$ data (*22*) (Fig. 3, A to C, and tables S2 and S3) show distinct variations in mass-independent fractionation of sulfur isotopes (MIF-S) among the different units. Sedimentary sulfides from bedded carbonates and volcanoclastic sandstones exhibit positive $\Delta^{33}S$ anomalies of 1.0 ± 0.6‰. By contrast, the bedded barite analyzed displays a negative $\Delta^{33}S$ value of −1.2‰, which is similar to that found in (*12*) ($\Delta^{33}S = -1.0 \pm 0.1$‰ for both bedded and vein barites). Most (95%) of the microscopic sulfides in bedded barite have positive $\Delta^{33}S$ anomalies of +2.3‰ ± 1.8. Intermediate to these, the macroscopic sulfide laminates (+0.4‰ ± 0.8) show both $+\Delta^{33}S$ and $-\Delta^{33}S$ anomalies. The presence of positive and negative $\Delta^{33}S$ anomalies indicates that the source of sulfur in the chert-barite unit had cycled through the atmosphere and was introduced to the ocean to be subsequently incorporated in the seafloor sediments as insoluble elemental sulfur (S^0, represented by sulfides in bedded carbonates and volcanoclastic sandstones) or deeper into the sedimentary succession as soluble sulfate (represented by barite in the bedded and vein barite).

The observed positive $\Delta^{33}S$ of the sedimentary sulfides (Fig. 3A), macroscopic sulfide laminates (Fig. 3B), and microscopic sulfides (Fig. 3C) requires reactions involving S^0. The initial $\delta^{34}S$ of S^0 that reached the ocean floor is unknown. This value can be constrained if we assume that the SO_2-photolysis array at UV radiation of wavelength 193 nm documented for the Early Archaean (*13*) can be used to establish the array on which both initial S^0 and SO_4 must lie (Fig. 1). We used the mean $\delta^{34}S$ (+4.7‰) and $\Delta^{33}S$ (−1.0‰) values of barite (fig. S2) (*1*, *12*, *23*) as a point of reference for the precise alignment of the theoretical 193-nm array (Fig. 3, A to C) and determined that the initial S^0 must have had a $\delta^{34}S$ between −3 and +3‰. Most sulfides with positive $\Delta^{33}S$ anomalies show a limited range of $\delta^{34}S$ values, with fractionation relative to the S^0 source between 0 and −7‰. These sulfides could have formed through abiologic reduction or disproportionation of elemental sulfur to sulfide

during hydrothermal alteration, which can produce $\delta^{34}S$ isotope fractionations of only a few per mil at temperatures below 300°C [<6‰ for S^0-FeS_2 reduction (*24*), and <3‰ for S^0 disproportionation (*25*)]. Alternatively, microbial reduction of elemental sulfur to H_2S, which does not produce notable isotopic fractionation (*26*), could also explain the negligible ^{34}S depletion of these sulfides.

The microscopic sulfides within the well-preserved barite crystals (zones 84-6, 89-3b, and two microscopic sulfides of zone 89-3a in drill core PDP2B; zone 96-6 of drill core PDP2C) have $\delta^{34}S$ and $\Delta^{33}S$ values that lie on a well-defined array (broken line in Fig. 3C) parallel to the experimentally determined 193-nm MIF-S array. This finding supports the view that the 193-nm radiation was the dominant UV source during the Early Archaean (*13*).

Other microscopic sulfides (fig. S1; zones 89-3a I, II, and III and zone 89.3b of drill core PDP2B) are depleted in $\delta^{34}S$ by as much as ~23‰ relative to the S^0 source (Fig. 3C). Most of these strongly ^{34}S-depleted microscopic sulfides show positive $\Delta^{33}S$ anomalies and therefore cannot be explained by microbial sulfate reduction, as they would necessarily display negative (SO_4-derived) $\Delta^{33}S$ anomalies, not positive (S^0-derived) $\Delta^{33}S$ anomalies. Based on the same line of reasoning, certain abiologic reactions can be ruled out as well. The reduction of SO_4 in the presence of a metal catalyst during low-temperature (<350°C) hydrothermal circulation (*24*) can lead to sulfides with a strong ^{34}S depletion. Such sulfides, however, would also inherit a negative $\Delta^{33}S$, not the observed positive $\Delta^{33}S$. Another abiologic process—low- to medium-temperature (<400°C) hydrolysis of SO_2 in relatively oxidizing magmatic fluids (*27*)—can be ruled out as well because it implies a common origin of the reaction products and therefore requires that both sulfides and surrounding sulfates display the same $\Delta^{33}S$ anomaly.

Three microscopic sulfides display a negative $\Delta^{33}S$ (zone 89-3a in drill core PDP2B) (Fig. 3C). These microscopic sulfides could be the product of microbial SO_4 reduction, abiologic SO_4 reduction associated with low-temperature hydrothermal circulation, or both. A microbial origin of such microscopic sulfides therefore cannot be ruled out but is controversial, and strongly depends on the inferred depositional environment: either shallow marine evaporite (*1*) or hydrothermal deposit (*28*).

Thus, microbial processes involving S^0 best explain the large range of $\delta^{34}S$ fractionations recorded by the microscopic sulfides with positive $\Delta^{33}S$ anomalies. As shown above, these $\delta^{34}S$ fractionations are higher than the range of fractionations observed for modern sulfur-reducing microbes (*26*). Microbial disproportionation of S^0 to H_2S and SO_4^{2-} can lead to a depletion in ^{34}S by up to 16‰, and most disproportionating organisms produce fractionations smaller than 8‰ (*11*, *29*). Consortia of different types of sulfur-metabolizing organisms (S^0 disproportionators versus H_2S oxidizers), however, could have driven the $\delta^{34}S$ down during repeated cycling of this S^0 source. Such a process is described by Canfield and Thamdrup (*30*) to explain the discrepancy between the isotopic compositions of sedimentary sulfides recorded in a broad range of environments and the known magnitude of fractionations produced by natural populations of sulfur processers. A qualitative model for $\delta^{34}S$ depletion by this process is shown in Fig. 4A. Sulfate produced during S^0 disproportionation would immediately react with Ca or Ba to form gypsum or barite, respectively. This biologically derived gypsum or barite with a positive $\Delta^{33}S$ anomaly inherited from parent elemental sulfur will be instantaneously mixed with a large reservoir of evaporative gypsum or hydrothermal barite with negative $\Delta^{33}S$ anomalies. The extent to which other intermediate sulfur species, such as $S_2O_3^{2-}$ and SO_3^{2-}, would have formed during this process is not clear (Fig. 4B). Microbial reduction or disproportionation of SO_3^{2-} can cause ^{34}S depletion as low as −33‰ (*31*, *32*) and −37‰ (*10*, *11*), respectively. We conclude, based on the overall positive $\Delta^{33}S$ of these microscopic sulfides, that the ultimate source for this metabolic sulfur-cycling was atmospherically derived S^0, not atmospherically derived SO_4. After reaching the ocean floor, insoluble particulate S^0 was incorporated in synsedimentary evaporitic gypsum (*1*) and/or hydrothermally emplaced barites (*28*). Such particles provided a solid substrate to which elemental sulfur disproportionators could attach (*33*) and use H_2, CH_4, or organic compounds as an electron donor to form H_2S (*9*, *34*). This H_2S could have been oxidized back to S^0 by biologic [e.g., anoxygenic photosynthesizers (*30*)] or abiologic reactions.

The basal positions of sulfur and sulfate metabolizers in the phylogenetic tree has led to the conclusion that these organisms could be among the most ancient of our ancestors (*9*, *34*, *35*). At present, no detailed information from gene sequencing is available for the deep branching in the phylogenetic tree of sulfur-disproportionating metabolism. The combined $\delta^{34}S$ and $\Delta^{33}S$ data presented here, however, support the early origin of this group of organisms. Although only this form of sulfur metabolism can be successfully traced in this Early Archaean environment, several

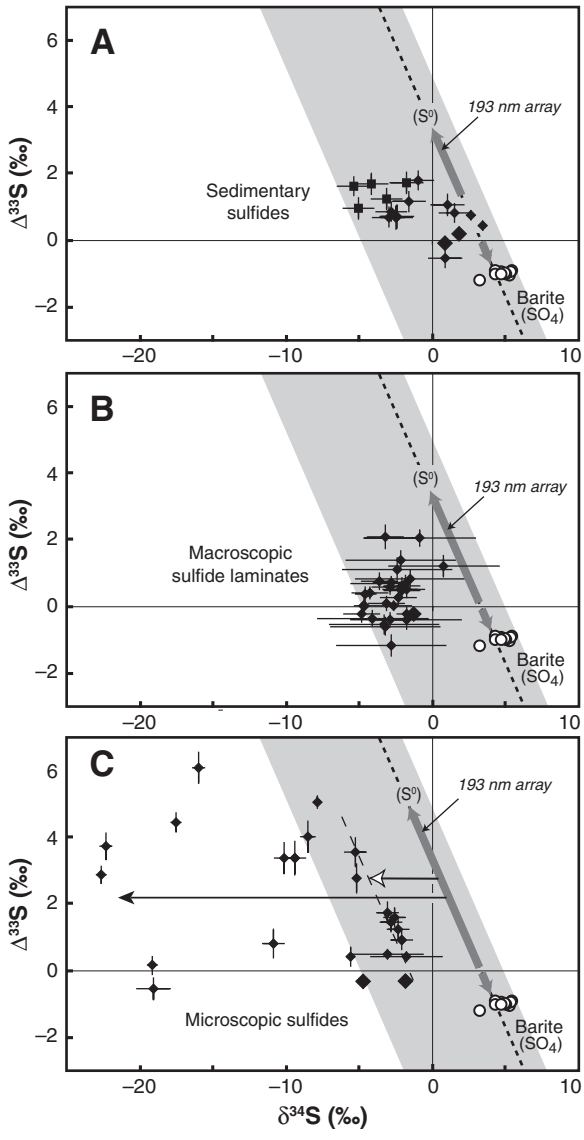

Fig. 3. Multiple–sulfur isotopic compositions of sulfides and sulfates of drillcore samples PDP2B and PDP2C. Variations of $\delta^{34}S$ with $\Delta^{33}S$ for individual sulfide analyses with the ion microprobe are shown as small symbols with 2σ error bars and for bulk barite and sulfide separates analyses as large symbols with error included in the symbol size. The 193-nm array refers to the UV-driven photolysis array at 193 nm defined in Fig. 1 (*13*) and is aligned by the mean $\delta^{34}S$ and $\Delta^{33}S$ values of North Pole barite. Bulk isotope analyses of barite [isolated white circle (this study) and cluster of white circles from (*12*)] are shown in all diagrams for comparison. (**A**) Sulfides from the sedimentary sequence [bedded carbonates (squares) and volcanoclastic sandstones (diamonds)]. (**B**) Macroscopic sulfide laminates mantling barite in bedded barite. (**C**) Microscopic sulfides in barite crystals from the bedded barite. The black arrow indicates the fractionation trend associated with microbial elemental sulfur disproportionation coupled to an inorganic or microbial oxidative metabolic pathway (see text). The white arrow points to fractionations produced by inorganic reduction or disproportionation, and/or microbial elemental sulfur reduction.

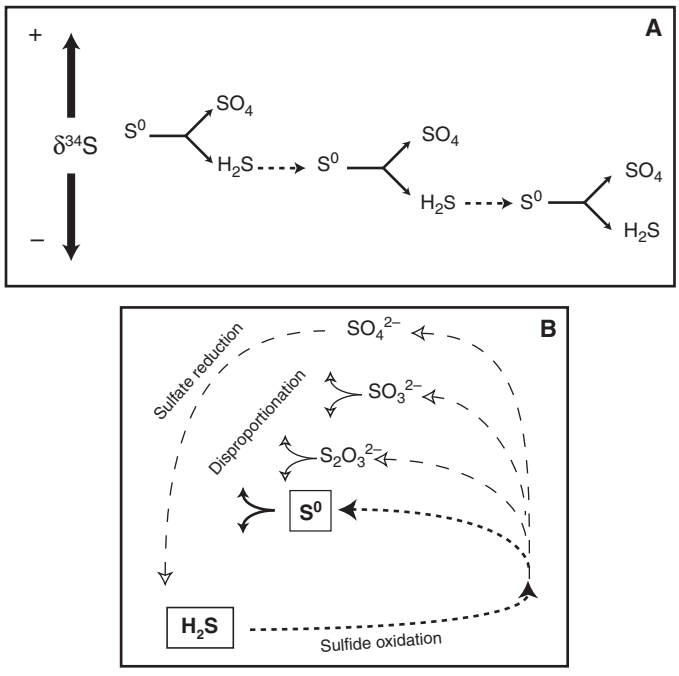

Fig. 4. Possible pathways of microbially mediated sulfur transformations and associated isotope fractionations based on (*11*) and (*30*). (**A**) Qualitative representation describing how S^0 disproportionation would lead to isotopically depleted H_2S and isotopically enriched SO_4. The H_2S that forms in this way can be reoxidized by inorganic processes or anoxygenic photosynthesizing organisms (*11*), leading to the formation of intermediate compounds such as S^0. The isotope fractionation associated with bacterial or inorganic oxidation of H_2S to S^0 is minor compared to S^0 disproportionation (*24*, *26*). Progressive disproportionation-oxidation steps will increase the ^{34}S depletion between H_2S and the initial S^0 reservoir by 20 to 30‰. (**B**) The role of other intermediate sulfur species such as $S_2O_3^{2-}$ and SO_3^{2-} in this Early Archaean environment is not clear, but it is possible that a complex consortium of sulfur-metabolizing organisms coexisted that included the cycling of these intermediate species. The three different disproportionation reactions involving S^0, $S_2O_3^{2-}$, and SO_3^{2-} are ($4S^0 + 4H_2O \rightleftharpoons 3H_2S + SO_4^{2-} + 2H^+$), ($S_2O_3^{2-} + H_2O \rightleftharpoons H_2S + SO_4^{2}$), and ($4SO_3^{2-} + 2H^+ \rightleftharpoons H_2S + 3SO_4^{2-}$) (*11*).

other forms of sulfur-based life could have been active at this time, including sulfide reducers, sulfide oxidizers, disproportionizers that used thiosulfate, or sulfite and sulfate reducers. Multiple–sulfur isotope analysis would be unable to trace the activity of elemental sulfur reducers. The preservation of a non–^{34}S-fractionated array of microscopic sulfides parallel to the 193-nm MIF-S array may be viewed as evidence for the early existence of S^0 reducers cohabitating with S^0 disproportionators.

References and Notes

1. Y. Shen, R. Buick, D. E. Canfield, *Nature* **410**, 77 (2001).
2. Y. Shen, R. Buick, *Earth Science Rev.* **64**, 243 (2004).
3. E. M. Cameron, *Nature* **296**, 145 (1982).
4. H. Ohmoto, T. Kakegawa, D. R. Lowe, *Science* **262**, 555 (1993).
5. D. E. Canfield, *Nature* **396**, 450 (1998).
6. D. E. Canfield, K. S. Habicht, B. Thamdrup, *Science* **288**, 658 (2000).
7. K. S. Habicht, M. Gade, B. Thamdrup, P. Berg, D. E. Canfield, *Science* **298**, 2372 (2002).
8. D. E. Canfield, *Geochim. Cosmochim. Acta* **65**, 1117 (2001).
9. K. O. Stetter, G. Gaag, *Nature* **305**, 309 (1983).
10. K. S. Habicht, D. E. Canfield, J. Rethmeier, *Geochim. Cosmochim. Acta* **62**, 2585 (1998).
11. D. E. Canfield, *Rev. Mineral. Geochem.* **43**, 607 (2001).
12. J. Farquhar, H. Bao, M. H. Thiemens, *Science* **289**, 756 (2000).
13. J. Farquhar, J. Savarino, S. Airieau, M. H. Thiemens, *J. Geophys. Res.* **106**, 32829 (2001).
14. J. Farquhar, B. A. Wing, *Earth Planet. Sci. Lett.* **213**, 1 (2003).
15. S. Ono *et al.*, *Earth Planet. Sci. Lett.* **213**, 15 (2003).
16. B. S. Kamber, M. Whitehouse, *Geobiology* **5**, 5 (2007).
17. R. I. Thorpe, A. H. Hickman, D. W. Davis, J. K. Mortensen, A. F. Trendall, in *The Archaean: Terrains, Processes and Metallogeny*, J. E. Glover, S. Ho, Eds. (University of Western Australia, Perth, 1992), vol. 22, pp. 395–408.
18. W. Nijman, K. C. H. De Bruijne, M. E. Valkering, *Precambrian Res.* **88**, 25 (1998).
19. M. J. Van Kranendonk, *Earth Sci. Rev.* **74**, 197 (2006).
20. R. Buick, J. S. R. Dunlop, *Sedimentology* **37**, 247 (1990).
21. Y. Ueno, H. Yoshioka, S. Maruyama, Y. Isozaki, *Geochim. Cosmochim. Acta* **68**, 573 (2004).
22. Materials and methods are available as supporting material on *Science* Online.
23. I. B. Lambert, T. H. Donnelly, J. S. R. Dunlop, D. I. Groves, *Nature* **276**, 808 (1978).
24. H. Ohmoto, M. B. Goldhaber, in *Geochemistry of Hydrothermal Ore Deposits* H. L. Barnes, Ed. (Wiley, New York, 1997), pp. 517–611.
25. J. W. Smith, *Geochem. J.* **34**, 95 (2000).
26. B. Fry, H. Gest, J. M. Hayes, *FEMS Microbiol. Lett.* **22**, 283 (1984).
27. R. O. Rye, *Chem. Geol.* **215**, 5 (2005).
28. B. Runnegar, W. A. Dollase, R. A. Ketcham, M. Colbert, W. D. Carlson, *Geol. Soc. Am.* (Abstr. 2001), p. 404A.
29. D. E. Canfield, B. Thamdrup, S. Fleischer, *Limnol. Oceanogr.* **43**, 253 (1998).
30. D. E. Canfield, B. Thamdrup, *Science* **266**, 1973 (1994).
31. A. G. Harrison, H. G. Thode, *Trans. Faraday Soc.* **54**, 84 (1958).
32. A. L. W. Kemp, H. G. Thode, *Geochim. Cosmochim. Acta* **32**, 71 (1968).
33. J. P. Amend, K. L. Rogers, D. R. Meyer-Dombard, in *Sulfur Biogeochemistry—Past and Present* J. P. Amend, K. J. Edwards, T. W. Lyons, Eds. (Geological Society of America, Boulder, CO, 2004), vol. 379, pp. 17–34.
34. K. O. Stetter, G. Fiala, G. Huber, R. Huber, G. Segerer, *Microbiol. Rev.* **75**, 117 (1990).
35. D. E. Canfield, R. Raiswell, *Am. J. Sci.* **299**, 697 (1999).
36. M. J. Van Kranendonk, P. Philippot, K. Lepot, *West. Aust. Geol. Surv. Rec.* **2006/14**, 25 (2006); available at www.doir.wa.gov.au/GSWA/publications.

37. We thank the Institut de Physique du Globe de Paris (IPGP), the Institut des Sciences de l'Univers, and the Geological Survey of Western Australia (GSWA) for supporting the Pilbara Drilling Project. P. Philippot, J. Farquhar, and M. Van Kranendonk acknowledge support from Programme National de Planétologie, Agence Nationale de la Recherche, NSF EAR Career Grant, and Australian Research Council Linkage International Program. Special thanks to P. Lopez-Garcia and D. Moreira for their participation in the Pilbara Drilling Project and for discussion; P. Rey and A. Dutkiewicz for discussion; and M. Chaussidon, C. Rollion-Bard, D. Mangin, O. Boudouma, and M. Fialin for assistance with ion mass spectrometry, scanning electron microscopy, and electron probe microanalyses. This is IPGP Contribution No. 2262, published with permission of the executive director of the GSWA.

Supporting Online Material

www.sciencemag.org/cgi/content/full/317/5844/1534/DC1
Materials and Methods
Figs. S1 and S2
Tables S1 to S3
References

30 May 2007; accepted 8 August 2007
10.1126/science.1145861

Current-Induced Magnetization Switching with a Spin-Polarized Scanning Tunneling Microscope

S. Krause,*§ L. Berbil-Bautista,*† G. Herzog, M. Bode,‡ R. Wiesendanger

Switching the magnetization of a magnetic bit by injection of a spin-polarized current offers the possibility for the development of innovative high-density data storage technologies. We show how individual superparamagnetic iron nanoislands with typical sizes of 100 atoms can be addressed and locally switched using a magnetic scanning probe tip, thus demonstrating current-induced magnetization reversal across a vacuum barrier combined with the ultimate resolution of spin-polarized scanning tunneling microscopy. Our technique allows us to separate and quantify three fundamental contributions involved in magnetization switching (i.e., current-induced spin torque, heating the island by the tunneling current, and Oersted field effects), thereby providing an improved understanding of the switching mechanism.

The increase of hard disk and memory capacities is a result of continuously decreasing bit sizes. For example, the area of one bit in today's magnetic hard disks is on the order of $(60\ nm)^2$. Two distinct effects are used to read and write information: The giant magnetoresistive effect is used for reading, whereas writing is done by a magnetic field. When exceeding a certain limit of bit density, however, switching the magnetization of one bit may also affect the